IAI Journals.ASM.org

Neutrophils Select Hypervirulent CovRS Mutants of M1T1 Group A *Streptococcus* during Subcutaneous Infection of Mice

Jinquan Li,[a,b] Guanghui Liu,[a] Wenchao Feng,[a] Yang Zhou,[a] Mengyao Liu,[a] James A. Wiley,[a] Benfang Lei[a]

Department of Microbiology and Immunology, Montana State University, Bozeman, Montana, USA[a]; College of Food Science and Technology, Huazhong Agricultural University, Wuhan, People's Republic of China[b]

Pathogen mutants arise during infections. Mechanisms of selection for pathogen variants are poorly understood. We tested whether neutrophils select mutations in the two-component regulatory system CovRS of group A *Streptococcus* (GAS) during infection using the lack of production of the protease SpeB (SpeB activity negative [SpeB^{A-}]) as a marker. Depletion of neutrophils by antibodies RB6-8C5 and 1A8 reduced the percentage of SpeB^{A-} variants (SpeB^{A-}%) recovered from mice infected with GAS strain MGAS2221 by >76%. Neutrophil recruitment and SpeB^{A-}% among recovered GAS were reduced by 95% and 92%, respectively, in subcutaneous MGAS2221 infection of CXCR2$^{-/-}$ mice compared with control mice. In air sac infection with MGAS2221, levels of neutrophils and macrophages in lavage fluid were reduced by 49% and increased by 287%, respectively, in CXCR2$^{-/-}$ mice compared with control mice, implying that macrophages play an insignificant role in the reduction of selection for SpeB^{A-} variants in CXCR2$^{-/-}$ mice. One randomly chosen SpeB^{A-} mutant outcompeted MGAS2221 in normal mice but was outcompeted by MGAS2221 in neutropenic mice and had enhancements in expression of virulence factors, innate immune evasion, skin invasion, and virulence. This and nine other SpeB^{A-} variants from a mouse all had nonsynonymous *covRS* mutations that resulted in the SpeB^{A-} phenotype and enhanced expression of the CovRS-controlled secreted streptococcal esterase (SsE). Our findings are consistent with a model that neutrophils select spontaneous *covRS* mutations that maximize the potential of GAS to evade neutrophil responses, resulting in variants with enhanced survival and virulence. To our knowledge, this is the first report of the critical contribution of neutrophils to the selection of pathogen variants.

The human pathogen group A *Streptococcus* (GAS) causes both relatively mild pharyngitis and superficial skin infections and potentially lethal, severe invasive infections (1). Severe invasive infections are most frequently caused by GAS strains of serotypes M1, M3, and M12 among GAS strains of >200 M protein serotypes in the United States (2). In particular, a serotype M1T1 clone of M1 GAS that emerged in the 1980s has globally disseminated and has been associated with the resurgence of severe invasive GAS infections in the last 30 years (3–11). Clinical isolates from severe invasive infections usually possess hypervirulence and an enhanced capacity to invade soft tissues and evade neutrophil responses compared with pharyngitis isolates (12–14). Invasive GAS isolates frequently carry a mutation in the genes encoding the two-component regulatory system CovRS (also known as CsrRS) (15, 16), and *covRS* mutations are a common cause of their hypervirulence and enhancement of soft tissue invasion and innate immune evasion (12–14). CovRS negatively regulates many virulence factors, including most of those that are involved in innate immune evasion (17–20). As a result of CovRS mutations, the loss of the production of the protease SpeB and enhanced production of the hyaluronic acid capsule and secreted streptococcal esterase (SsE) contribute to the phenotype of hypervirulent isolates (14, 21–25).

The association of the M1T1 GAS clone with severe invasive infections appears to be linked to its proneness to the selection of *covRS* mutations during infection. A natural *covS* deletion in an invasive M1T1 isolate is responsible for its hypervirulence and enhanced innate immune evasion (14). Null *covS* mutations of M1T1 isolates arise in experimental invasive infection in mice (12, 26, 27). The lack of production of the protease SpeB (SpeB^{A-}, for the SpeB activity-negative phenotype) has been used as a marker for GAS variants with *covRS* mutations (27, 28), although the validity of this approach has not been rigorously tested. In contrast, the first sequenced M1 GAS strain, SF370, rarely switches to the SpeB^{A-} phenotype during experimental mouse infection (27). The DNase Sda1, encoded by a prophage, which is carried by some M1T1 isolates but not by SF370, plays a critical role in the selection of *covRS* mutations of M1T1 isolate 5448 during infection in mice (27). However, introduction of the Sda1-encoding prophage into SF370 does not facilitate the selection of SpeB^{A-} mutants *in vivo* (29). Furthermore, hypervirulent variants with *covS* mutations arise in strains that lack Sda1 (30). Besides Sda1, the capsule synthetase gene *hasA* and the M protein gene *emm* are required for the selection of SpeB^{A-} variants (28). Despite these considerable efforts and advancement, the exact basis for the selection of *covRS* mutants *in vivo* remains unknown.

In contrast to the active search for the basis on the pathogen side for the selection of *covRS* mutations, there has been no report on host factors that contribute to the selection of CovRS mutants. Here we report the first examination of the role of host factors in the selection of GAS *covRS* mutations. We found that neutrophils are the primary selection pressure for *covRS* mutants of M1T1 GAS strain MGAS2221. We also demonstrated that a randomly

Received 14 November 2013 **Returned for modification** 26 November 2013
Accepted 17 January 2014
Published ahead of print 22 January 2014
Editor: L. Pirofski
Address correspondence to Benfang Lei, blei@montana.edu.

doi:10.1128/IAI.01458-13
The authors have paid a fee to allow immediate free access to this article.

chosen isolate with a null *covS* mutation had an advantage in survival and an enhanced capacity to evade innate immune responses. These findings demonstrate that neutrophils critically contribute to the selection of M1T1 GAS *covRS* mutations that compromise neutrophil responses and enhance GAS survival and virulence.

MATERIALS AND METHODS

Declaration of ethical approval. All animal experimental procedures were carried out in strict accordance with the recommendations in the *Guide for the Care and Use of Laboratory Animals* (31). The protocols for the experiments were approved by the Institutional Animal Care and Use Committee at Montana State University (permit number 2011-57).

Bacterial strains and growth. Sequenced M1 isolate SF370 (32) and M1T1 strain MGAS2221 (12) were used in this study. SpeB^{A-} strain 1 (SpeB^{A-1}) was a randomly chosen mutant among isolates that were recovered from MGAS2221 skin infection sites in mice and had abolished SpeB production. This strain had a deletion of 5 bases at positions 132 to 136 of the *covS* gene. These GAS isolates and other testing strains were grown in Todd-Hewitt broth supplemented with 0.2% yeast extract (THY) at 37°C in 5% CO_2. Tryptose agar with 5% sheep blood and THY agar were used as the solid media. GAS bacteria used for animal experiments were harvested at the mid-exponential growth phase (optical density at 600 nm [OD_{600}] of 0.4) and washed three times with and resuspended in pyrogen-free Dulbecco's phosphate-buffered saline (DPBS) to the desired doses.

Neutrophil depletion. Rat anti-murine Ly6G monoclonal antibodies (MAbs) RB6-8C5 and 1A8 and isotype control MAb 2A3 for 1A8 were purchased from Bio X Cell. To deplete and maintain the depletion of neutrophils, 250 μg RB6-8C5 or 1A8 in 0.5 ml DPBS was injected into the intraperitoneal cavity of each female C57BL/6 mouse (5 weeks old) at 24 h prior to and 24 h after GAS inoculation. Control mice were treated similarly with 2A3 or DPBS. The efficiency of neutrophil depletion was evaluated by flow cytometry analysis. Blood samples were collected into heparinized tubes from maxillary bleeds of mice 24 h after they had been treated with RB6-8C5, 1A8, or the control. The blood samples were incubated with an antibody cocktail of fluorescein isothiocyanate (FITC)-conjugated rat anti-mouse CD11b (BD Biosciences) and Alexa Fluor 647-conjugated rat anti-mouse Ly6G (BioLegend) at a 1:200 dilution at 37°C for 15 min. Red blood cells in the samples were then lysed by using the Whole Blood Lysing Reagent kit (Beckman Coulter) according to the manufacturer's protocol. White blood cells in the stained samples were analyzed on a BD LSR flow cytometer running FACSDiva software (BD Biosciences). Flow cytometry data were analyzed by using the FlowJo software program (TreeStar Inc.). Levels of neutrophils at skin infection sites 24 h after GAS inoculation were also determined, as described below, to confirm the efficiency of neutrophil depletion.

Mouse infections. Selection of SpeB^{A-} variants was done by using 5-week-old female C57BL/6 neutropenic mice, male CXCR2 knockout (KO) (CXCR2$^{-/-}$) mice in the BALB/c background, and BALB/c control mice for CXCR$^{2-/-}$ mice. These mice were bred at the Animal Resource Center at Montana State University using breeding pairs of mice from the Jackson Laboratory (Bar Harbor, ME). The CXCR2$^{-/-}$ mice [C.129S2(B6)-*Cxcr2*^{tm1Mwm}/J] had a deficiency in chemokine (C-X-C) receptor 2 and impaired neutrophil migration (33). Each mouse was subcutaneously inoculated with 0.2 ml of an MGAS2221 or SF370 suspension at an OD_{600} of 0.9. In experiments using neutropenic mice, GAS was inoculated subcutaneously in mice 24 h after mice were injected intraperitoneally with 250 μg RB6-8C5 or 1A8, and the mice were injected with the antibodies again at 24 h after GAS infection. The infection site in the skin was collected at the indicated times after inoculation to measure the percentage of SpeB^{A-} variants (SpeB^{A-}%) of GAS bacteria isolated from these tissues.

Five-week-old female CD-1 mice from Charles River Laboratories were used to compare the SpeB^{A-1} strain with MGAS2221 in virulence, neutrophil recruitment, skin invasion, and systemic GAS dissemination. Groups of 15 mice were subcutaneously inoculated with 0.2 ml of MGAS2221 and SpeB^{A-1} suspensions in DPBS at an OD_{600} of 0.9. Five mice of each group were euthanized to collect skin samples for measurement of lesion size and neutrophil recruitment as described below, and the liver and spleen were also harvested to measure numbers of viable GAS bacteria. The other 10 mice of each group were monitored daily for 14 days to determine survival rates.

Quantification of SpeB^{A-} isolates. The skin and liver samples obtained as described above were homogenized in DPBS by using a Kontes pestle and plated at appropriate dilutions. Forty-eight colonies were randomly picked from each sample, inoculated in 200 μl THY in 96-well plates, and cultured overnight. Three microliters of 10% β-mercaptoethanol was added to each well, and the cultures in the plate were centrifuged at 3,500 rpm. The SpeB activity in the supernatant of GAS cultures grown overnight was detected by using a casein plate assay as described previously (34).

Cytospin analysis. MGAS2221 (0.1 ml of bacterial suspension in DPBS with an OD_{600} of 1.1) was injected with 0. 9 ml air subcutaneously into 5 male BALB/c (control) or CXCR2$^{-/-}$ mice. Twelve hours later, the mice were euthanized, and the air sac of each mouse was lavaged with 1 ml of cold DPBS. An aliquot of the recovered lavage fluid was used to determine the total number of live cells by trypan blue exclusion counts. A second aliquot of the recovered lavage fluid at an appropriate dilution was used to prepare cytospin slides using a Shandon Cytospin cytocentrifuge. The slides were stained by using the Diff-Quik stain kit from Fisher Scientific. Neutrophils and macrophages among 150 host cells on each cytospin slide were counted to determine the percentages of neutrophils and macrophages, and the total numbers of neutrophils and macrophages were calculated from the percentage data and the total counts of live cells in the lavage samples.

GAS competitive growth/survival assay. A 1:1 SpeB^{A-1}-MGAS2221 mixture (0.2 ml) was injected with 0.8 ml air subcutaneously into 18 C57BL/6 or neutropenic mice obtained from C57BL/6 mice by treatment with MAb RB6-8C5. Nine C57BL/6 or neutropenic mice were euthanized at 1 h or 24 h after inoculation, and the air sac was lavaged with 1 ml PBS. The lavage samples were plated onto THY agar plates. The percentage of SpeB^{A-1} variants in GAS colonies for each lavage sample was determined by analyzing 48 colonies of each sample with an SpeB activity assay, as described above. SpeB^{A-1} and MGAS2221 showed negative and positive SpeB production, respectively.

Quantification of neutrophil infiltration. The skin around the infection site was peeled off, and the skin lesion was recognized by the boundary of the inflammation area. The size of skin lesions was measured by analyzing the lesion pictures using the area measurement tool of the Adobe Acrobat 9 software program (Adobe Systems Inc.). The skin containing the infection area was excised for neutrophil measurement. Numbers of recruited neutrophils in the infected skin samples were determined by a myeloperoxidase assay, as described previously (35).

DNA sequencing. A DNA fragment containing the *covRS* genes was amplified from test strains by using the primers 5′-TCGCTAGAAGACTATTTGAC-3′ and 5′-TTCATGTCATCCATCATTGC-3′ and the Phusion high-fidelity PCR kit (New England BioLabs). DNA sequencing of the amplified PCR products was performed by using the BigDye Terminator v3.1 cycle sequencing kit and an Applied Biosystems 3130 genetic analyzer. Primers used for sequencing were 5′-TCGCTAGAAGACTATTTGAC-3′, 5′-TTCATGTCATCCATCATTGC-3′, 5′-AACGGCTTCATCATATTTCC-3′, 5′-AAATCCACAAAACCGTTCAG-3′, 5′-TGATACACACGACCGATAG-3′, 5′-TTGATGACAGAAAGGGCAG-3′, 5′-TACGCGAACCATGTCTAAC-3′, and 5′-GTTGGGGTAAAGATGACAG-3′. Sequence data were analyzed by using Sequencer 5.1 software (Gene Codes Corporation).

Real time RT-PCR analysis. MGAS2221 and SpeB^{A-1} were grown at 37°C (5% CO_2) to an OD_{600} of 0.2 in THY. Total RNA was isolated from these GAS bacteria as described previously (24). High RNA quality was

confirmed by using an Agilent 2100 Bioanalyzer and an RNA 6000 Lab Chip kit (Agilent Technologies). TaqMan quantitative reverse transcription-PCR (RT-PCR) assays were performed by using probes specific for *emm*, *hasA*, *spyCEP*, *sse*, and *gyrA* (control) and the ABI 7500 Fast system (Applied Biosystems Inc.), as described previously (24). Control reaction mixtures that did not contain reverse transcriptase revealed no contamination of genomic DNA in any RNA sample. All RNA samples were assayed in triplicate, and mRNA levels of genes were compared by using the $\Delta\Delta C_T$ method with normalization to the mRNA levels of the *gyrA* gene, which were about the same in all samples.

Analyses for SsE production. Relative levels of SsE production by MGAS2221 and its variants were determined by Western blotting and the 2-thio-PAF hydrolysis assay (36) for platelet-activating factor acetylhydrolase (PAF-AH) activity in culture supernatants. Western blotting to detect the presence of SsE and Spy0469 (control), a secreted protein, in culture supernatants was performed as described previously (24). In the 2-thio-PAF hydrolysis assay, 100 μl of the culture supernatant from the exponential growth phase (OD_{600} = ~0.33) was mixed with 30 μl of a reactant solution containing 0.9 mM 2-thio-PAF and 1.3 mM 5,5′-dithiobis(2-nitrobenzoic acid) at room temperature in a well of a 96-well plate. The absorbance change at 414 nm (ΔA_{414}), as a measure of SsE-catalyzed 2-thio-PAF hydrolysis, was recorded with time by using a SPECTRA^{Max} 384 Plus spectrophotometer (Molecular Devices).

Complementation of CovRS mutants. Plasmid pCovSC for in *trans* complementation and the vector control pDCBB were described previously (20). To construct the suicide plasmid pGRV-CovRS, a DNA fragment containing the *covRS* genes was amplified by using primers 5′-GGACAAGCTTTGAAATAGTCTAGGATATGAG-3′ and 5′-GCGGATCCTGGTAGATAGAGACCGCGTCA-3′, and the PCR product was cloned into pGRV (37) at the BglII and BamHI sites. SpeB^{A-} variants with *covS* mutations were transformed with pCovSC or pDCBB (20). For complementing SpeB^{A-} variants with *covR* mutations, pGRV-CovRS was integrated into the genome of the variants by a single crossover. All complement and vector control strains were selected with 10 mg/liter chloramphenicol.

Statistical analyses. The Prism software program (Graph-Pad Software Inc.) was used for all statistical analyses. Survival data were analyzed by using the log-rank (Mantel-Cox) test. The data in Fig. 1B and 5A were analyzed by using one-way analysis of variance (ANOVA) with Tukey's multiple-comparison test. The *P* values other than that in the survival study were obtained by using the two-tailed Mann-Whitney *t* test.

RESULTS

Time course of *in vivo* accumulation of MGAS2221 SpeB^{A-} variants. We hypothesize that GAS SpeB^{A-} variants are selected for better survival against innate immunity during infection. If this hypothesis is correct, SpeB^{A-} variants should accumulate with time. Thus, we measured the percentage of SpeB^{A-} variants of MGAS2221 among GAS bacteria recovered from infection sites in the skin at different time points after inoculation by analyzing 48 colonies from each mouse using the casein hydrolysis assay for the SpeB protease activity in the supernatants of cultures grown overnight (Fig. 1A). All colonies analyzed were confirmed to be GAS by their beta-hemolytic activity on blood agar plates, and GAS isolates with the SpeB^{A-} phenotype were analyzed twice and could be repeated. No SpeB^{A-} isolates were detected at 24 h after inoculation of MGAS2221, an M1T1 isolate. On day 2, the percentage (mean ± standard deviation [SD]) of SpeB^{A-} variants was 5.5% ± 8.1%, which increased to 17.9% ± 22.5% and 33.0% ± 19.5% on days 3 and 4, respectively (Fig. 1B). The data at one time point were significantly different from those 2 days apart. As reported previously (27), no SpeB^{A-} variants of GAS strain SF370 were detected at day 4 after GAS inoculation in mice (Fig. 1B). The total CFU of GAS at the MGAS2221 infection site remained nearly constant, ranging from 1.1×10^8 to 1.7×10^8 during a period of 4 days (Fig. 1C). However, the data showing that one-third of GAS bacteria on day 4 were SpeB^{A-} variants indicate active growth and clearance of GAS at infection sites.

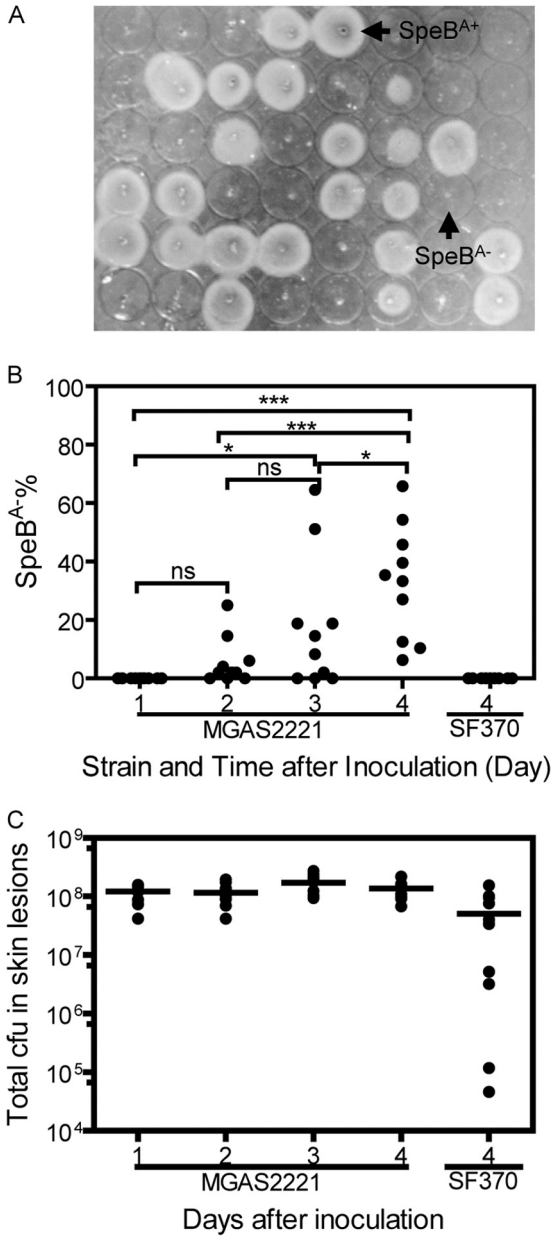

FIG 1 Time course of accumulation of SpeB^{A-} variants and number of GAS bacteria at skin infection sites. (A) Representative picture of the casein SpeB protease activity assay showing the presence (SpeB^{A+}) and absence (SpeB^{A-}) of SpeB activity in the culture supernatants of 48 GAS isolates from a mouse at day 4 after subcutaneous MGAS2221 infection. (B) SpeB^{A-}% among GAS bacteria recovered at skin infection sites of C57BL/6 mice at days 1 to 4 after subcutaneous inoculation with 2.5×10^7 CFU of MGAS2221 or at day 4 after inoculation with 2.0×10^7 CFU of SF370. ns, not significant. (C) Total numbers of viable GAS bacteria at the skin infection site of MGAS2221 as a function of time after inoculation in panel B. The data for SF370 at day 4 after infection are included in panels B and C for comparison. Asterisks indicate significance, with *** showing more significance than *. ns, not significant.

Neutrophils exert pressure for selection of SpeB^{A-} variants. We next tested whether neutrophils exert primary pressure for

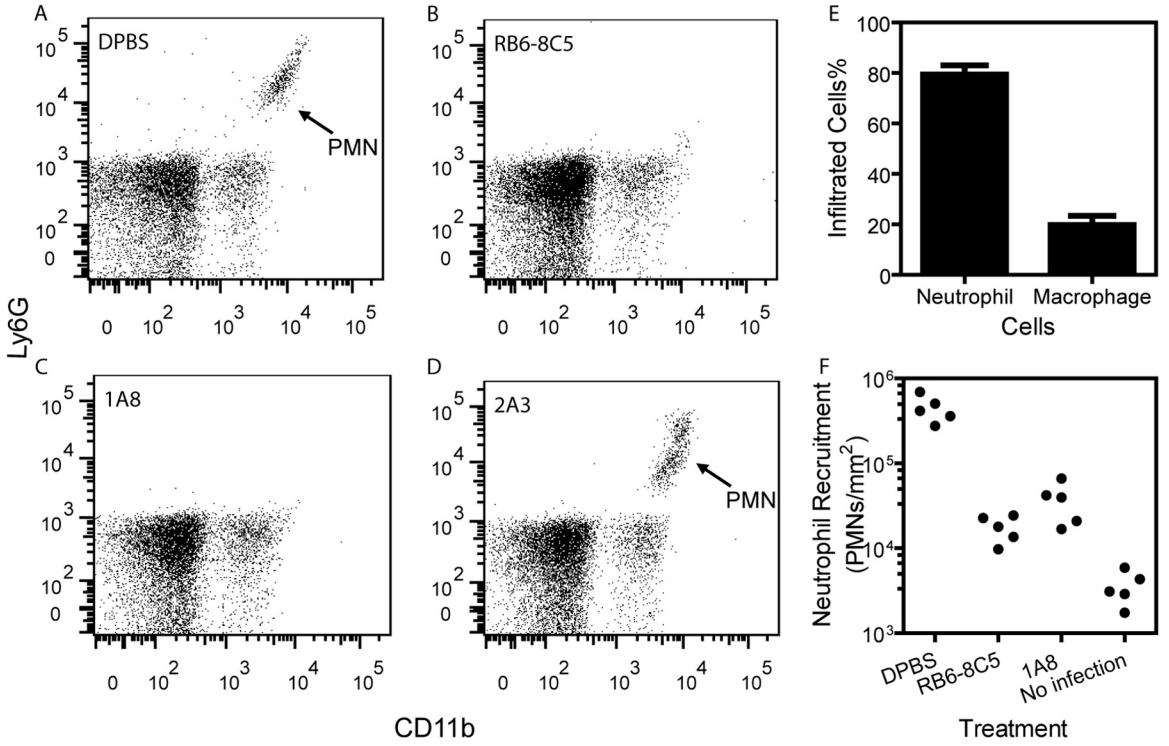

FIG 2 Assessment of the efficiency of neutrophil depletion in mice treated with monoclonal antibody RB6-8C5 or 1A8. Neutrophil depletion and sample preparation are described in Materials and Methods. (A to D) FACS analyses of $Ly6G^+/CD11b^+$ neutrophils among all white cells from mice that were treated with DPBS (A), RB6-8C5 (B), 1A8 (C), or 2A3 (D). (E) Percentages of neutrophils and macrophages at the skin infection site of MGAS2221 at 24 h after inoculation. The numbers of neutrophils and macrophages were counted among 150 cells by examining H&E-stained skin samples under a microscope. (F) Levels of infiltrated neutrophils at the infection site in the skin at 24 h after inoculation of 9.4×10^7 CFU MGAS2221 in C57BL/6 mice. The mice were intraperitoneally injected with DPBS, RB6-8C5, or 1A8 at 24 h prior to MGAS2221 infection. PMN, polymorphonuclear leukocytes.

selection of $SpeB^{A-}$ variants. We first used neutropenic mice to address this question. To obtain neutropenic mice, 250 μg of monoclonal antibody RB6-8C5, which was commonly used to deplete mice of neutrophils (38), was injected into the intraperitoneal cavity. The efficiency of neutrophil depletion was examined by fluorescence-activated cell sorting (FACS). Blood was collected 24 h after the RB6-8C5 treatment, and white blood cells were incubated with Alexa Fluor-labeled anti-Ly6G and FITC-labeled anti-CD11b antibodies. FACS analysis detected $Ly6G^+/CD11b^+$ neutrophils in the blood of DPBS-treated (control) but not RB6-8C5-treated mice (Fig. 2A and B). To determine whether the RB6-8C5 treatment reduces the levels of neutrophils at infections sites, RB6-8C5-treated and DPBS-treated mice were infected subcutaneously with MGAS2221 24 h after RB6-8C5 injection, and levels of neutrophils at skin infection sites were measured 24 h after GAS injection by using the myeloperoxidase assay (35). Because monocytes also produce myeloperoxidase at levels from 33% of those in neutrophils in human (39) to 1.8% of those in neutrophils in rats (35), we first estimated the contribution of inflammatory macrophages to levels of myeloperoxidase at the skin infection sites 24 h after MGAS2221 inoculation. Percentages of neutrophils and macrophages among 150 cells at hematoxylin and eosin (H&E)-stained skin infection sites were 80% and 20%, respectively (Fig. 2E). Using the relative myeloperoxidase contents in human monocytes compared to those in neutrophils, 33%, for the relative myeloperoxidase content in mouse monocytes relative to that in mouse neutrophils, the contribution of monocytes to myeloperoxidase levels at the MGAS2221 skin infection site would be about 7%. Since mouse is more closely related to rat than human, mouse monocytes might contribute <7% of myeloperoxidase at MGAS2221 skin infection sites. Thus, the myeloperoxidase assay is a reasonably valid approach to estimate the levels of neutrophils at the skin infection site for infection of mice with MGAS2221. Using this assay, the infection site in the control mice had $(4.5 \pm 1.6) \times 10^5$ neutrophils/mm^2, whereas the infection site in RB6-8C5-treated mice had $(1.8 \pm 0.6) \times 10^4$ neutrophils/mm^2, representing a 96% reduction in recruited neutrophils at infection sites in the RB6-8C5-treated mice (Fig. 2F). The neutrophil depletion was maintained during the 5-day experiment by a second injection of RB6-8C5 at 24 h after GAS inoculation.

MGAS2221 bacteria were recovered from the skin infection sites on day 4 after inoculation and were analyzed to determine whether they produced SpeB by the SpeB protease activity assay (34). Dead mice were excluded from the SpeB activity assay. A total of (1.5 ± 2.0)% of GAS bacteria recovered from RB6-8C5-treated mice did not produce SpeB, whereas (53 ± 26)% of GAS bacteria recovered from DPBS-treated mice had the $SpeB^{A-}$ phenotype ($P = 0.0009$) (Fig. 3A). The treatment of mice with RB6-8C5 nearly abolished the selection of $SpeB^{A-}$ variants during infection.

Because RB6-8C5 also depletes a subset of monocytes that express granulocyte receptor 1 (Gr1) (38), the results of the RB6-8C5 experiment would indicate a role of neutrophils and/or inflammatory macrophages in the selection of $SpeB^{A-}$ variants

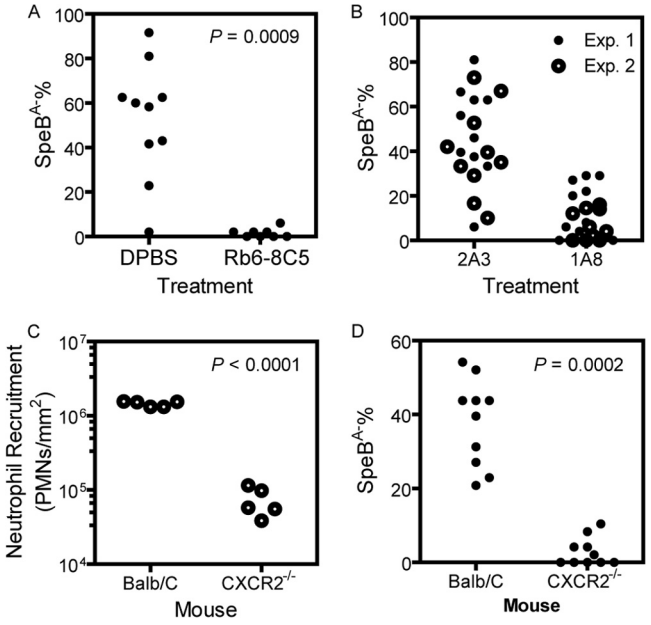

FIG 3 Neutrophils select SpeB^{A-} variants. (A and B) SpeB^{A-}% of GAS isolates recovered from the skin infection site of MGAS2221 in C57BL/6 mice with intraperitoneal treatment with DPBS or RB6-8C5 (A) and 2A3 (subtype MAb control) or 1A8 (B) at day 4 post-subcutaneous infection with 5×10^7 CFU of MGAS2221. (C) Levels of neutrophil infiltration at the skin infection site of MGAS2221 in BALB/c and CXCR2$^{-/-}$ mice at 24 h postinoculation. (D) SpeB^{A-}% of GAS isolates recovered from the skin infection site in BALB/c and CXCR2$^{-/-}$ mice at day 4 post-subcutaneous infection with MGAS2221.

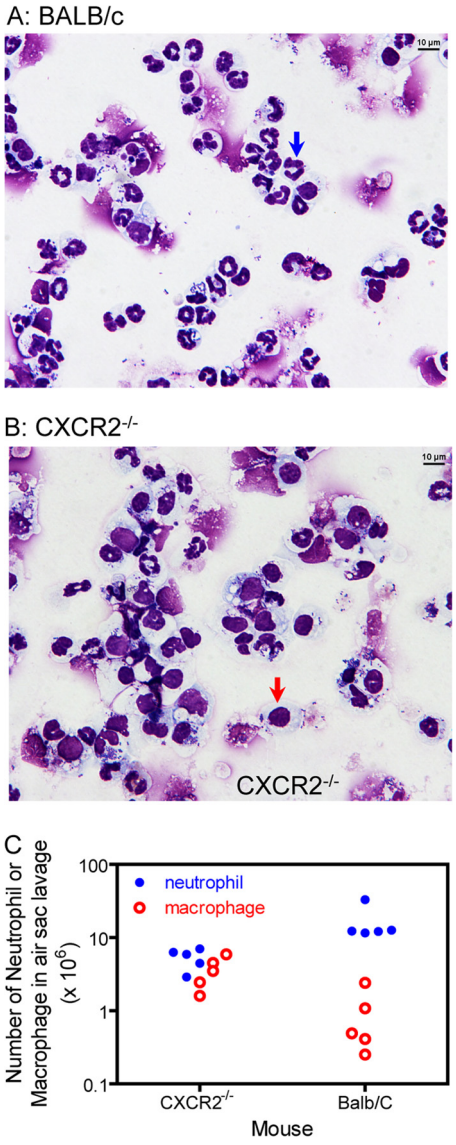

FIG 4 Comparison of neutrophil and macrophage infiltration in air sac MGAS2221 infection of CXCR2$^{-/-}$ and BALB/c mice by cytospin analysis. Air sacs containing MGAS2221 were lavaged at 12 h after GAS inoculation, and neutrophils and macrophages in the lavage fluid were quantified as described in Materials and Methods. (A and B) Representative pictures of cytospin showing neutrophils (blue arrow) and macrophages (red arrow) for the lavage samples from BALB/c (A) and CXCR2$^{-/-}$ (B) mice. (C) Numbers of neutrophils and macrophages in the lavage samples from BALB/c and CXCR2$^{-/-}$ mice.

during infection. We performed two additional tests to further examine the role of neutrophils in SpeB^{A-} selection. First, the anti-Ly6G-specific MAb 1A8, which targets only neutrophils (38), was used to deplete neutrophils. FACS analyses showed that treatment with 1A8 (Fig. 2E), but not 2A3 (subtype control MAb) (Fig. 2D), efficiently depleted neutrophils. The myeloperoxidase assay showed that 1A8 reduced neutrophil levels at MGAS2221 infection sites by 92% compared with DPBS-treated mice (Fig. 2F), and this reduction efficiency was slightly lower than that for the RB6-8C5 treatment. The percentages of SpeB^{A-} isolates among GAS bacteria recovered from 1A8-treated mice in two independent experiments (experiment 1, 14% ± 12%; experiment 2, 7% ± 7%; combined, 11% ± 10%) were significantly lower than those recovered from mice treated with 2A3 (experiment 1, 49% ± 21%; experiment 2, 40% ± 20%; combined, 46% ± 21%) (P values of 0.0011 [experiment 1], 0.0001 [experiment 2], and <0.0001 [combined]) (Fig. 3B). The results indicate a major role of neutrophils in the selection of SpeB^{A-} variants.

The second experiment used CXCR2$^{-/-}$ mice. These mice have impaired neutrophil migration (33). MGAS2221 induced $(7.3 \pm 3.2) \times 10^4$ neutrophils/mm^2 at subcutaneous infection sites in CXCR2$^{-/-}$ mice, which was only 5% of that at infection sites in BALB/c mice ($[1.45 \pm 0.12] \times 10^6$ neutrophils/mm^2) ($P <$ 0.0001) (Fig. 3C). The SpeB^{A-}% for GAS bacteria recovered from skin infection sites of MGAS2221 in CXCR2$^{-/-}$ mice was 2.9% ± 3.8%, which was only 7.6% of that for GAS bacteria from BALB/c mice (38.0% ± 12%) ($P = 0.0002$) (Fig. 3D). It is possible that CXCR2$^{-/-}$ mice reduced the recruitment of inflammatory macrophages due to the impaired neutrophil infiltration during MGAS2221 infection, resulting in a reduction in the selection of SpeB^{A-} variants. To examine this possibility, we quantified the numbers of neutrophils and macrophages in the lavage fluid of the skin air sac containing MGAS2221 at 12 h after inoculation in CXCR2$^{-/-}$ and BALB/c (control) mice. More than 90% of host cells were neutrophils in the lavage fluid from BALB/c mice (Fig. 4A and C), whereas macrophages constituted 40% of host cells in the lavage fluid from CXCR2$^{-/-}$ mice (Fig. 4B and C). The CXCR2$^{-/-}$ mouse lavage fluid had a 67% reduction in neutrophil numbers ($P = 0.0079$) and a 290% increase in macrophage numbers ($P = 0.0159$) compared to the BALB/c lavage fluid (Fig. 4C). If inflammatory macrophages play a critical role in the selection of SpeB^{A-} variants, CXCR2$^{-/-}$ mice should have lower macrophage

infiltration during MGAS2221 infection since the SpeB^{A-}% of GAS isolates recovered from CXCR2$^{-/-}$ mice was lower than that from control mice. Thus, the increase in macrophage infiltration in infection of CXCR2$^{-/-}$ mice rules out a major role of inflammatory macrophages in the selection of SpeB^{A-} variants of MGAS2221. Taken together, all the results of the three experiments indicate that neutrophils play a dominant role in the selection of MGAS2221 SpeB^{A-} variants during infection.

Advantage in survival and disadvantage in growth of the SpeB^{A-1} strain compared to the parent strain. The role of neutrophils in the selection of SpeB^{A-} variants suggests that the mutants may be more resistant to neutrophil-mediated clearance than MGAS2221. To test this idea, we performed a competitive growth/clearance assay in normal and neutropenic mice. The neutropenic mice were prepared by depletion of neutrophils with RB6-8C5, as described above. RB6-8C5 was used for this test was because the test was performed immediately after we observed the detrimental effect of the RB6-8C5 treatment of mice on the selection for SpeB^{A-} variants of MGAS2221 during infection and before 1A8 was used later for additional tests. In this competitive assay, an approximate 1:1 mixture of SpeB^{A-1}, a randomly chosen SpeB^{A-} mutant, and MGAS2221 was subcutaneously inoculated into C57BL/6 mice without (normal mice) or with (neutropenic mice) depletion of neutrophils, and 24 h later, viable bacteria were recovered from infection sites to determine SpeB^{A-}% in the recovered SpeB^{A-1}-MGAS2221 mixture. The number of SpeB^{A-} variants derived from MGAS2221 at 24 h after inoculation should be negligible according to the data in Fig. 1B. Indeed, sequencing of the *covRS* genes in 10 randomly picked SpeB^{A-} colonies from this competitive assay found that they had the same *covS* mutation as SpeB^{A-1}. Thus, the SpeB^{A-}% data in this test reflected the relative growth and survival of SpeB^{A-1} and MGAS2221 in both normal and neutropenic mice. The percentage of SpeB^{A-1} variants in GAS in neutropenic mice significantly decreased from 66% ± 8% at 1 h after inoculation to 55% ± 8% at 24 h after inoculation ($P = 0.0213$) (Fig. 5A). These data indicate that the relative population of SpeB^{A-1} decreased with time in neutropenic mice and that SpeB^{A-1} grew more slowly than MGAS2221 *in vivo*. The growth rate of SpeB^{A-1} in THY was 75% of that of MGAS2221 according to the slope of the growth curves in the exponential growth phase (Fig. 5B). In contrast, the percentage of SpeB^{A-1} bacteria in GAS from normal mice significantly increased from 70% ± 6% at 1 h after inoculation to 83% ± 13% at 24 h after inoculation ($P = 0.0133$) (Fig. 5A). The SpeB^{A-1}% value at 24 h after inoculation in normal mice was 51% higher than that in neutropenic mice ($P = 0.0006$). The data show that the relative population of SpeB^{A-1} bacteria increased with time in normal mice. Thus, even though SpeB^{A-1} had a disadvantage in growth *in vivo* compared to MGAS2221, it had a survival advantage over the parent strain against innate immune responses. The data suggest that SpeB^{A-} mutants are selected because of their advantage for survival against innate immunity over the parent strain.

Enhanced innate immune evasion by SpeB^{A-1}. SpeB^{A-} variants must have enhanced innate immune evasion to have an advantage in survival over the parent strain. To test this possibility, a mouse model of subcutaneous infection was used to compare SpeB^{A-1} to MGAS2221 in levels of neutrophil infiltration, skin invasion, systemic dissemination, and virulence. Levels of neutrophils at the MGAS2221 infection site at 24 h postinoculation

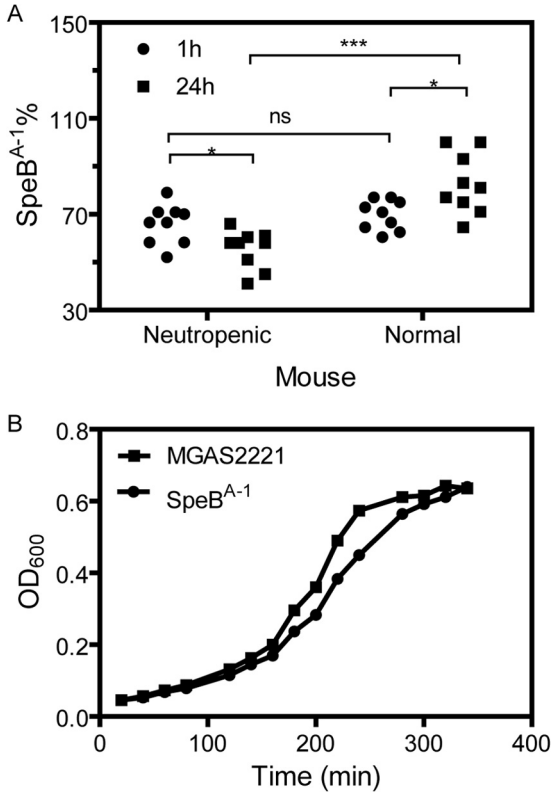

FIG 5 Survival advantage and growth disadvantage of SpeB^{A-1} compared to wild-type MGAS2221. (A) Percentage of SpeB^{A-1} variants at 1 h and 24 h after inoculation of an SpeB^{A-1}-MGAS2221 mixture in a mouse model of air sac infection. The data are for mice (9 mice per group) treated with RB6-8C5 (neutropenic mice) and DPBS (normal mice). (B) Growth curves of MGAS2221 and SpeB^{A-1} in THY. Asterisks indicate significance, with *** showing more significance than *. ns, not significant.

(mean value ± SD of [1.1 ± 0.3] × 10^5 neutrophils/mm^2) were 5.6-fold higher than those at the SpeB^{A-1} infection site ([1.9 ± 0.8] × 10^4 neutrophils/mm^2) ($P = 0.0004$) (Fig. 6A). The lesion size caused by SpeB^{A-1} infection (406 ± 155 mm^2) was 3-fold greater than that caused by MGAS2221 (131 ± 28 mm^2) ($P = 0.0045$) (Fig. 6B). Numbers of viable GAS bacteria in the liver and spleen of mice infected with SpeB^{A-1} at 24 h after inoculation were (1.2 ± 1.6) × 10^5 CFU/g and (6.5 ± 12) × 10^7 CFU/g, respectively, whereas very few GAS bacteria were detected in the liver and spleen of mice infected by MGAS2221 (Fig. 6C and D). In the survival test, all mice infected with SpeB^{A-1} did not survive, but all mice infected with MGAS2221 did ($P < 0.0001$) (Fig. 6E). Thus, SpeB^{A-1} had a higher capacity than MGAS2221 to evade neutrophil responses, invade the skin tissue, and disseminate, resulting in the hypervirulence of the mutant.

SpeB downregulation and SsE upregulation in SpeB^{A-} variants were caused by *covRS* mutations. The phenotype of SpeB^{A-1} described above was similar to that of GAS isolates from human patients and mice that have null *covS* mutations (12–14). Indeed, DNA sequencing of the *covRS* genes revealed that SpeB^{A-1} had a deletion of bases 132 to 136 of the *covS* gene (5′-TTTCT-3′). Transcription of the innate immunity-evading genes *hasA*, *spyCEP*, and *sse* in SpeB^{A-1} was enhanced by >35-fold compared with MGAS2221 (Fig. 6F). These results are consistent with pre-

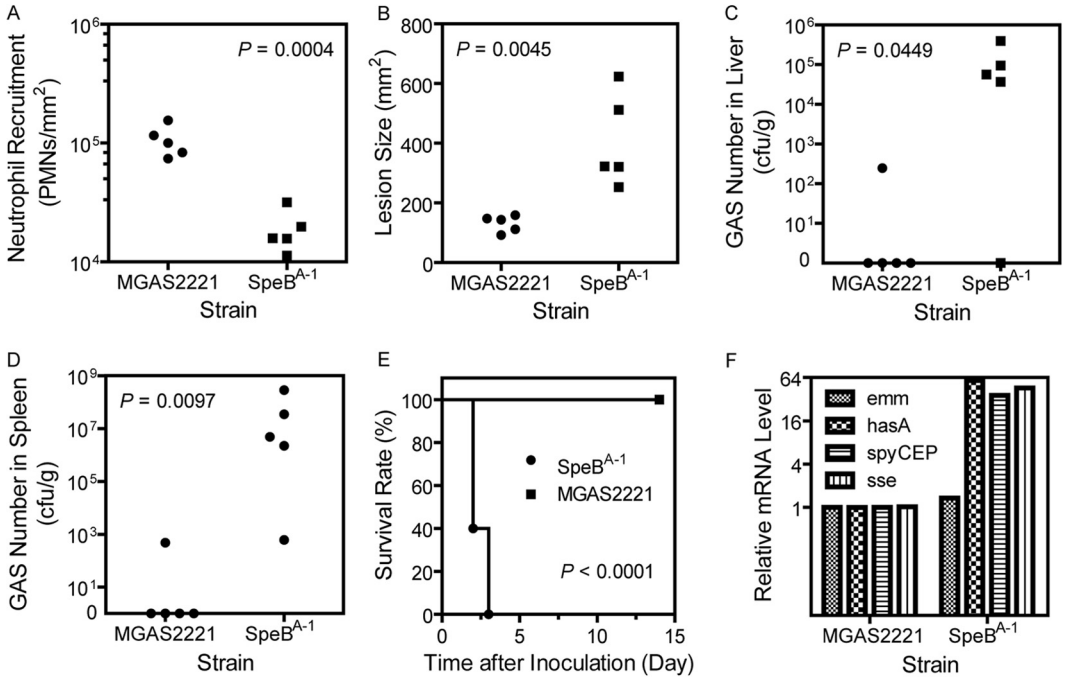

FIG 6 The SpeB^{A-1} isolate displays enhancement in innate immune evasion, skin evasion, systemic dissemination, virulence, and expression of virulence factors. (A to D) Neutrophil recruitment (A), lesion size (B), and numbers of viable GAS bacteria in the liver (C) and spleen (D) at 24 h after subcutaneous inoculation of 9.0×10^7 CFU MGAS2221 or 8.5×10^7 CFU SpeB^{A-1} in female CD1 mice. (E) Survival curves of CD1 mice after subcutaneous infection with the same dose of MGAS2221 and SpeB^{A-1}. (F) Relative mRNA levels of the *emm*, *hasA*, *spyCEP*, and *sse* genes in SpeB^{A-1} at an OD_{600} of 0.2 compared with MGAS2221.

vious findings on the effect of null *covS* deletion on expression of these virulence genes (14, 24).

To determine whether *covRS* mutations were common among SpeB^{A-} variants of MGAS2221 recovered from mice, we sequenced the *covRS* genes of all 11 SpeB^{A-} isolates and 2 randomly chosen SpeB^{A+} colonies among 48 tested GAS colonies from a mouse. All 11 SpeB^{A-} variants had *covRS* mutations: 6 of them with a deletion, insertion, or nonsense mutation that resulted in the truncation of CovS; 3 variants with an Ala-to-Asp missense mutation at position 388 of CovS (CovS^{Ala388Asp}); and 2 variants with CovR^{Ile205Phe} mutations (Table 1). In contrast, both SpeB^{A+} isolates had the wild-type *covRS* sequence. In addition, there were no synonymous mutations in the *covRS* genes of the 11 SpeB^{A-} variants, indicating that the *covRS* mutations were selected.

We next checked the SsE expression of the 11 SpeB^{A-} variants as an indicator of whether these *covRS* mutants enhanced expression of virulence genes. SsE solely confers the enzymatic activity of hydrolyzing platelet-activating factor (PAF) in GAS culture supernatants, and the PAF hydrolysis activity increases when the *covS* gene is deleted or has a null mutation (14, 25, 36). The PAF hy-

TABLE 1 CovRS mutations and *in vitro* SsE expression of SpeB^{A-} variants of MGAS2221 isolated from subcutaneous mouse infection[c]

Strain[a]	*covRS* mutation	Mutated CovS or CovR	SpeB production	*In vitro* SsE[b] production
1	^{132}TTTCT^{136} deletion in *covS*	Truncated CovS	−	+
2	^{223}G to T in *covS*	Truncated CovS	−	+
3	^{1166}C to A in *covS*	CovS^{Ala388Asp}	−	+
4	^{481}C to T in *covS*	Truncated CovS	−	+
5	Insertion of ATTTTCTCTGC at nucleotide 99 in *covS*	Truncated CovS	−	+
6	^{616}A to T in *covR*	CovR^{Ile205Phe}	−	+
7	^{616}A to T in *covR*	CovR^{Ile205Phe}	−	+
8	^{1166}C to A in *covS*	CovS^{Ala388Asp}	−	+
9	^{1363}C to T in *covS*	Truncated CovS	−	+
10	^{1363}C to T in *covS*	Truncated CovS	−	+
11	^{1166}C to A in *covS*	CovS^{Ala388Asp}	−	+
12	None	wt	+	−
13	None	wt	+	−
14	wt	wt	+	−

[a] Strains 1 through 11 were all SpeB^{A-} variants detected among 48 randomly chosen colonies isolated from a mouse infected with MGAS2221, and strains 12 and 13 were randomly chosen from 37 SpeB^{A+} colonies in the same test. Strain 14 was MGAS2221.
[b] The SsE production status was assigned according to the data shown in Fig. 7.
[c] wt, wild type.

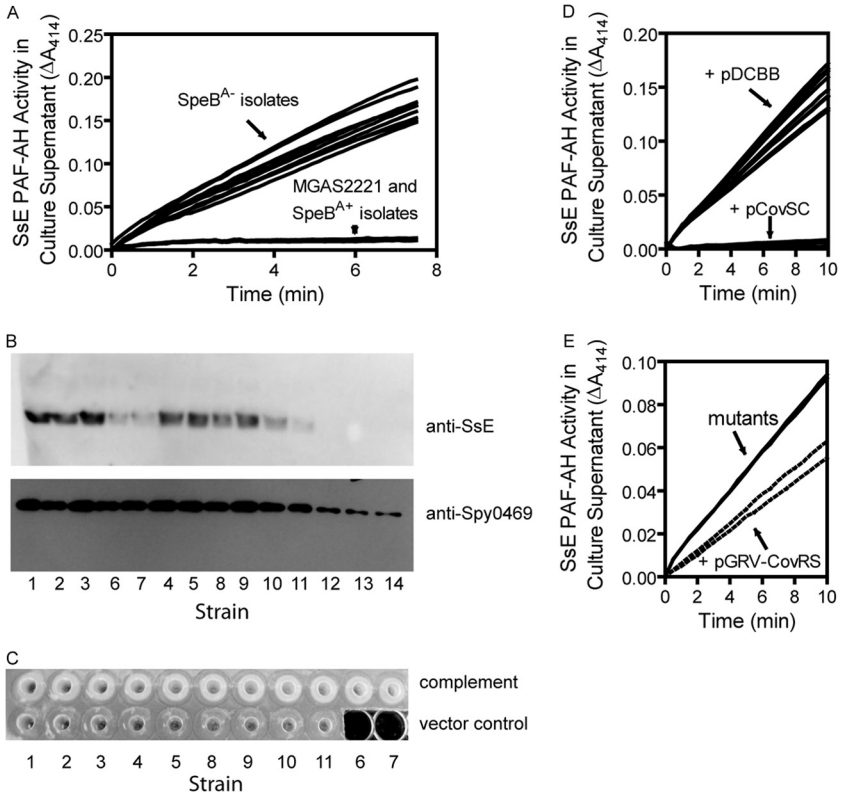

FIG 7 The SpeB^{A-}/SsE^{A+} phenotype of *in vivo*-selected MGAS2221 variants is caused by *covRS* mutations. (A) SsE PAF acetylhydrolase activity in the culture supernatant of SpeB^{A-} variants with *covS* mutations and SpeB^{A+} isolates from MGAS2221-infected mice. (B) Western blots for SsE and Spy0469 (control) in culture supernatants showing positive detection of SsE in SpeB^{A-} variants (strains 1 through 11) but not in SpeB^{A+} isolates (strains 12 and 13) and MGAS2221 (strain 14). (C) Complementation of SpeB^{A-} variants with pGRV-CovRS (strains 6 and 7) and pCovSC (the other strains) converted the SpeB^{A-} phenotype of the mutants into the SpeB^{A+} phenotype, and pDCBB controls for pCovSC did not change the status of SpeB production. Strain numbers correspond to those in Table 1. (D) SsE PAF-AH activity in the culture supernatant of pDCBB (control)- and pCovSC-transformed SpeB^{A-} variants with *covS* mutations listed in Table 1. (E) SsE PAF-AH activity in culture supernatants of the two CovR mutants and their complemented strains with integrated pGRV-CovRS.

drolysis activity of SsE was very low in the culture supernatants of MGAS2221 and two SpeB^{A+} isolates at the mid-log growth phase (designated the SsE^{A-} phenotype) but substantially increased in the culture supernatants of the SpeB^{A-} variants (designated the SsE^{A+} phenotype) (Fig. 7A and D). These results were confirmed by the presence and absence of SsE in the culture supernatants of SpeB^{A-} and SpeB^{A+} isolates, respectively, by Western blotting, whereas Spy0469 (control) was detected in all the culture supernatants (Fig. 7B). Thus, the SpeB^{A-} variants with the *covRS* mutations all had enhanced SsE expression.

To determine whether the *covRS* mutations caused the SpeB^{A-}/SsE^{A+} phenotype of these SpeB^{A-} variants, these mutants were complemented with wild-type *covS* or *covRS*. The strains with the *covS* mutations were transformed with plasmid pCovSC, whereas the suicide plasmid pGRV-CovRS was integrated into the genomes of the two isolates with the CovR^{Ile205Phe} mutation. The complemented strains of these *covRS* mutants all restored SpeB production, whereas the vector controls still had the Spe^{A-} phenotype (Fig. 7C). The complementation of the nine SpeB^{A-} variants with *covS* mutations reduced SsE activity in the culture supernatants to the levels of MGAS2221 (Fig. 7D). The complemented *covR* mutants reduced SsE production but still had significantly higher SsE activity than MGAS2221 (Fig. 7E), which might be caused by the presence of a single copy of both the wild-type and mutated *covR* alleles in the complement strains. These results indicate that the observed *covRS* mutations are responsible for the SpeB^{A-}/SsE^{A+} phenotype.

DISCUSSION

This report presents two findings on the role of neutrophils in the selection of hypervirulent CovRS mutants of an M1T1 isolate during subcutaneous infection of mice. First, neutrophils play a critical role in the selection of CovRS mutants. Second, CovRS mutants of MGAS2221 are selected for better survival, even though they have a disadvantage in growth *in vivo* compared with wild-type MGAS2221. The significance of these findings is 2-fold. First, these findings are consistent with a model in which neutrophil responses mount pressure for the selection of spontaneous CovRS mutations that enhance innate immune evasion and consequently confer to GAS better survival under the attack of neutrophils. Second, these findings will facilitate the elucidation of the genetic variations among GAS isolates that dictate whether SpeB^{A-} mutants are selected during soft tissue infections.

Null *covS* mutation-carrying M1T1 strains from severe invasive infection or mouse passage are SpeB^{A-} strains (12–14, 20). The SpeB^{A-} phenotype of such a strain has been shown to be caused by a null *covS* mutation (14). Conversely, characterized M1T1 SpeB^{A-} variants from mouse passage have null *covS* muta-

tions (13, 23, 27). SpeB^{A-} variants have been used to quantify *covRS* mutations in mouse passage (27, 28), which was apparently based on the assumption that the selected SpeB^{A-} phenotype is caused by *covRS* mutations. All 11 SpeB^{A-} variants obtained from the same mouse had *covRS* mutations, and the SpeB^{A-}/SsE^{A+} phenotype of these variants was caused by the *covS* or *covR* mutations. Thus, our data appear to validate the approach that uses the SpeB^{A-} phenotype as a marker to screen for and quantify *covRS* mutations of M1T1 isolates during passage in mice. Our data also show that, besides *covS* truncation mutations, *covS* and *covR* missense mutations can lead to the SpeB^{A-}/SsE^{A+} phenotype. Certain *covS* missense mutations have been shown to enhance the production of NADase and reduce SpeB production (40), and the CovS^{Ala388Asp} mutation that causes the SpeB^{A-}/SsE^{A+} phenotype has not been reported. In addition, the CovR^{Ile205Phe} mutation has not been reported but is close to the known Arg203Ser and Gln216Pro mutations in the DNA-binding domain of CovR (41, 42). CovR^{Arg119His} confers a SpeB^{A-} phenotype (20), and CovR^{Ile205Phe} is the second CovR mutation that has been shown to cause the SpeB^{A-} phenotype.

A novel finding of this study is that neutrophils are required for the selection of CovRS mutations. Recruited macrophages play a role in clearance of GAS (43). However, macrophages appear not to play a critical role in the selection of *covRS* mutations in MGAS2221, since the decrease in the selection of SpeB^{A-} variants of MGAS2221 in CXCR2$^{-/-}$ mice is correlated with the impaired neutrophil recruitment but not with the increased levels of macrophages. These results imply that CovRS mutations confer advantages against the clearance of GAS by neutrophils but not by macrophages. This implication is supported by the fact that most of the known innate immunity-evading factors of GAS target neutrophils. Neutrophil infiltration is reduced by interleukin-8 (IL-8)/CXC chemokine peptidase SpyCEP (44–46), C5a peptidase ScpA (47), and platelet-activating factor acetylhydrolase SsE (14, 25). GAS produces the hyaluronic acid capsule and the major surface protein M to resist phagocytosis by neutrophils (48, 49). Neutrophils can also be destroyed by streptolysins S and O (50–52). Specific antibody-mediated opsonophagocytosis is inhibited by the secreted protein Mac (53). GAS also produces DNases to help it escape neutrophils' DNA-derived extracellular traps (54). All of these virulence factors except for the M protein and ScpA are regulated by CovRS. All these studies suggest that neutrophils mount critical innate immune responses against GAS, which is supported by a number of studies examining GAS killing by neutrophils (55–59).

The SpeB^{A-1} mutant outcompetes wild-type bacteria in mice with normal innate immune responses but is outcompeted by wild-type bacteria when neutrophils and inflammatory macrophages are depleted. These observations suggest that the accumulation of SpeB^{A-} mutants with time during infection is due to their advantage in survival against innate immune responses over wild-type bacteria, even though the mutants have a disadvantage in growth. Previous findings on the role of Sda1 in and the requirement of the *hasA* and *emm* gene for the selection of SpeB^{A-} mutants imply a survival advantage of SpeB^{A-} mutants *in vivo* (27, 28). Our findings explicitly demonstrate that *covS* mutants can survive better than the parent GAS strain in the presence of neutrophils and inflammatory macrophages. In addition, the ability of GAS to survive against neutrophil killing is more critical than the capacity of GAS to grow faster for the selection of CovRS mutants.

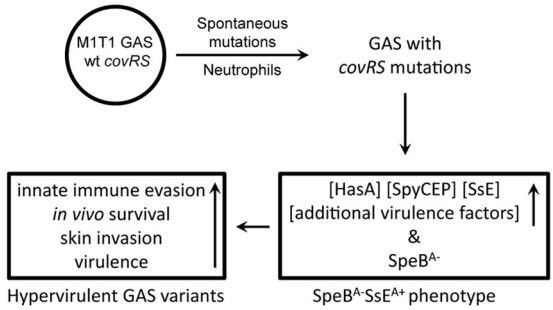

FIG 8 Model for *in vivo* selection of hypervirulent M1T1 GAS CovRS mutants. Neutrophils select spontaneous *covRS* mutations that enhance expression of multiple virulence genes and abolish SpeB production, resulting in mutants with enhanced innate evasion, *in vivo* survival, skin invasion, and virulence.

The survival advantage of CovRS mutants over wild-type GAS is apparently due to the enhanced innate immune evasion by the mutants. This advantage appears to be the reason for the *in vivo* accumulation of SpeB^{A-} variants of MGAS2221 with time, which is also observed for M1T1 strain 5448 (60). Consistent with previous findings (14, 61), SpeB^{A-1} had enhanced expression of IL-8/CXC chemokine peptidase SpyCEP and platelet-activating factor acetylhydrolase SsE as a result of the *covS* deletion. A null *covS* deletion not only reduces neutrophil recruitment but also keeps neutrophils away from GAS, and SsE critically contributes to this *covS* deletion-caused severe innate immune evasion (14, 25). It is possible that CovRS mutants could generate a local neutrophil-free zone through the action of SsE and SpyCEP. The enhanced production of the capsule and Sda1 can also contribute to the survival advantage by enhancing the resistance of GAS to phagocytosis and help mutants escape neutrophil extracellular trap-enhanced clearance, respectively (27).

The *covRS* mutations in the analyzed SpeB^{A-} variants were all nonsynonymous mutations and caused the SpeB^{A-}/SsE^{A+} phenotype. No *covRS* mutations were found in the sequenced SpeB^{A+} isolates. These observations indicate that the *covRS* mutations are selected. Our findings support a model for the occurrence of SpeB^{A-}/SsE^{A+} *covRS* mutants of M1T1 GAS strains during infection in which spontaneous *covR* or *covS* mutations are selected by neutrophils in soft tissue infections for an advantage against the innate immune system over parent strains with functional CovRS (Fig. 8). The new information in this study extends our current understanding that *covRS* mutations occur in clinical isolates and experimental animal infections and enhance innate immune evasion, skin invasion, and virulence.

The selection power for MGAS2221 *covRS* mutations in murine skin infections is striking. Our SpeB^{A-} data are consistent with data reported by Sumby et al. for mucoid isolates obtained from MGAS2221 in murine skin infections (12). Another M1T1 strain, 5448, readily switches to the SpeB^{A-} phenotype in skin infection as well (21, 27). These data for animal models of GAS infections appear to correlate with the fact that invasive isolates frequently have *covRS* mutations (15, 16). For example, the invasive M1T1 isolate MGAS5005 has a single-base deletion at position 83 in *covS*, and this 1-base deletion causes the hypervirulence and SpeB^{A-} phenotype of MGAS5005 (14). The sequenced

MGAS315 and MGAS6180 genomes have CovS^{G457V} and CovS^{G226E} mutations, respectively, compared with CovS of the sequenced M1 strain SF370 (32, 62, 63). In addition, the well-known virulent strains NZ131 and CS101 are also SpeB^{A-} strains (data not shown). However, not all GAS isolates switch to the SpeB^{A-} phenotype, and the *in vivo* selection of SpeB^{A-} variants appears to be associated with GAS strains that are linked to severe invasive infections. This would explain why we frequently obtain SpeB^{A+} isolates from human infections. MGAS2221 was isolated from a patient with scarlet fever and presumably from tonsil or pharynx (20). If true, the isolation of the SpeB^{A+} MGAS2221 strain would suggest that strains of the M1T1 clone associated with severe invasive infections may be subject to less selection pressure for SpeB^{A-} variants at the pharynx and tonsil than in soft tissues. As for the carriage stage, strains with wild-type *covRS* may eventually prevail because they do not divert a significant amount of energy to synthesize high levels of virulence factors that should not be needed when acute inflammation is gone. Indeed, the SpeB^{A-1} isolate with the null *covS* mutation grows slower both *in vivo* and *in vitro* than MGAS2221. MGAS5005, which has a natural *covS* deletion and SpeB^{A-} phenotype, grows slower *in vitro* than MGAS2221 (14). Tatsuno et al. recently also reported slower growth of *covS* mutants than strains with the wild-type *covS* gene (40). The slowdown in growth of *covS* mutants in comparison with wild-type strains could be the basis for the overgrowth of wild-type bacteria over *covS* mutants in saliva (20). Diversion of energy to the enhanced expression of CovRS-regulated virulence factors is most likely responsible for the slowdown in growth of SpeB^{A-} mutants both *in vitro* and *in vivo*.

Sda1 has been shown to provide selection pressure for SpeB^{A-} variants of M1T1 isolate 5448 (27). However, recent studies suggest that Sda1 does not play a direct and essential role in the selection of SpeB^{A-} variants. M1 isolate SF370 does not switch to an SpeB^{A-} phenotype (27), and the introduction of the Sda1-encoding phage into SF370 does not result in the selection of SpeB^{A-} variants during infection (29). Furthermore, serotype M98 GAS apparently undergoes SpeB^{A-} mutations in patients even though it lacks prophage-encoded Sda1 (30). Besides Sda1, the *hasA* and *emm* genes are also required for the selection of SpeB^{A-} variants of the M1T1 isolate (28). Both the hyaluronic acid capsule and M protein are required for resistance of GAS to phagocytosis by neutrophils. The loss of *hasA* or *emm* may cause a loss of the survival advantage conferred by *covRS* mutations. SF370 has functioning *hasA* and *emm* genes. Therefore, *hasA* and *emm* are required for but are not the direct cause of the selection of SpeB^{A-} variants. Thus, the exact basis for why *covRS* mutations are selected in strains of the M1T1 GAS clone associated with severe invasive infections but not the SF370 M1 isolate remains unknown. Since neutrophils exert pressure for the selection of CovRS mutants, identifying molecular events in the M1T1 clone that may lead to a disadvantage against neutrophil responses may be a good strategy to elucidate the basis for *in vivo* selection of *covRS* mutations.

ACKNOWLEDGMENTS

This work was supported in part by NIH grants AI095704 and AI097703 from the National Institute of Allergy and Infectious Diseases and GM103500-09 from the National Institute of General Medical Sciences, the USDA Formula Fund, and the Montana State University Agricultural Experimental Station. J.L. was supported by a Ph.D. student exchange scholarship of the Ministry of Education, China.

REFERENCES

1. **Carapetis JR, Steer AC, Mulholland EK, Weber M.** 2005. The global burden of group A streptococcal diseases. Lancet Infect. Dis. **5:**685–694. http://dx.doi.org/10.1016/S1473-3099(05)70267-X.
2. **O'Loughlin RE, Roberson A, Cieslak PR, Lynfield R, Gershman K, Craig A, Albanese BA, Farley MM, Barrett NL, Spina NL, Beall B, Harrison LH, Reingold A, Van Beneden C, Active Bacterial Core Surveillance Team.** 2007. The epidemiology of invasive group A streptococcal infection and potential vaccine implications: United States, 2000-2004. Clin. Infect. Dis. **45:**853–862. http://dx.doi.org/10.1086/521264.
3. **Musser JM, Hauser AR, Kim MH, Schlievert PM, Nelson K, Selander RK.** 1991. Streptococcus pyogenes causing toxic-shock-like syndrome and other invasive diseases: clonal diversity and pyrogenic exotoxin expression. Proc. Natl. Acad. Sci. U. S. A. **88:**2668–2672. http://dx.doi.org/10.1073/pnas.88.7.2668.
4. **Cleary PP, Kaplan EL, Handley JP, Wlazlo A, Kim MH, Hauser AR, Schlievert PM.** 1992. Clonal basis for resurgence of serious Streptococcus pyogenes disease in the 1980s. Lancet **339:**518–521. http://dx.doi.org/10.1016/0140-6736(92)90339-5.
5. **Musser JM, Kapur V, Kanjilal S, Shah U, Musher DM, Barg NL, Johnston KH, Schlievert PM, Henrichsen J, Gerlach D, Rakita RM, Tanna A, Cookson BD, Huang JC.** 1993. Geographic and temporal distribution and molecular characterization of two highly pathogenic clones of Streptococcus pyogenes expressing allelic variants of pyrogenic exotoxin A (scarlet fever toxin). J. Infect. Dis. **167:**337–346. http://dx.doi.org/10.1093/infdis/167.2.337.
6. **Martin DR, Single LA.** 1993. Molecular epidemiology of group A streptococcus M type 1 infections. J. Infect. Dis. **167:**1112–1117. http://dx.doi.org/10.1093/infdis/167.5.1112.
7. **Seppälä H, Vuopio-Varkila J, Osterblad M, Jahkola M, Rummukainen M, Holm SE, Huovinen P.** 1994. Evaluation of methods for epidemiologic typing of group A streptococci. J. Infect. Dis. **169:**519–525. http://dx.doi.org/10.1093/infdis/169.3.519.
8. **Musser JM, Kapur V, Szeto J, Pan X, Swanson DS, Martin DR.** 1995. Genetic diversity and relationships among Streptococcus pyogenes strains expressing serotype M1 protein: recent intercontinental spread of a subclone causing episodes of invasive disease. Infect. Immun. **63:**994–1003.
9. **Chatellier S, Ihendyane N, Kansal RG, Khambaty F, Basma H, Norrby-Teglund A, Low DE, McGeer A, Kotb M.** 2000. Genetic relatedness and superantigen expression in group A streptococcus serotype M1 isolates from patients with severe and nonsevere invasive diseases. Infect. Immun. **68:**3523–3534. http://dx.doi.org/10.1128/IAI.68.6.3523-3534.2000.
10. **Sumby P, Porcella SF, Madrigal AG, Barbian KD, Virtaneva K, Ricklefs SM, Sturdevant DE, Graham MR, Vuopio-Varkila J, Hoe NP, Musser JM.** 2005. Evolutionary origin and emergence of a highly successful clone of serotype M1 group A Streptococcus involved multiple horizontal gene transfer events. J. Infect. Dis. **192:**771–782. http://dx.doi.org/10.1086/432514.
11. **Aziz RK, Kotb MZ.** 2008. Rise and persistence of global M1T1 clone of Streptococcus pyogenes. Emerg. Infect. Dis. **14:**1511–1517. http://dx.doi.org/10.3201/eid1410.071660.
12. **Sumby P, Whitney AR, Graviss EA, DeLeo FR, Musser JM.** 2006. Genome-wide analysis of group A streptococci reveals a mutation that modulates global phenotype and disease specificity. PLoS Pathog. **2:**e5. http://dx.doi.org/10.1371/journal.ppat.0020005.
13. **Kansal RG, Datta V, Aziz RK, Abdeltawab NF, Rowe S, Kotb M.** 2010. Dissection of the molecular basis for hypervirulence of an in vivo-selected phenotype of the widely disseminated M1T1 strain of group A Streptococcus bacteria. J. Infect. Dis. **201:**855–865. http://dx.doi.org/10.1086/651019.
14. **Li J, Zhu H, Feng W, Liu M, Song Y, Zhang X, Zhou Y, Bei W, Lei B.** 2013. Regulation of inhibition of neutrophil infiltration by the two-component regulatory system CovRS in subcutaneous murine infection with group A streptococcus. Infect. Immun. **81:**974–983. http://dx.doi.org/10.1128/IAI.01218-12.
15. **Ikebe T, Ato M, Matsumura T, Hasegawa H, Sata T, Kobayashi K, Watanabe H.** 2010. Highly frequent mutations in negative regulators of multiple virulence genes in group A streptococcal toxic shock syndrome isolates. PLoS Pathog. **6:**e1000832. http://dx.doi.org/10.1371/journal.ppat.1000832.
16. **Shea PR, Beres SB, Flores AR, Ewbank AL, Gonzalez-Lugo JH, Martagon-Rosado AJ, Martinez-Gutierrez JC, Rehman HA, Serrano-Gonzalez**

M, Fittipaldi N, Ayers SD, Webb P, Willey BM, Low DE, Musser JM. 2011. Distinct signatures of diversifying selection revealed by genome analysis of respiratory tract and invasive bacterial populations. Proc. Natl. Acad. Sci. U. S. A. **108:**5039–5044. http://dx.doi.org/10.1073/pnas.1016282108.

17. **Levin JC, Wessels MR.** 1998. Identification of csrR/csrS, a genetic locus that regulates hyaluronic acid capsule synthesis in group A Streptococcus. Mol. Microbiol. **30:**209–219. http://dx.doi.org/10.1046/j.1365-2958.1998.01057.x.
18. **Heath A, DiRita VJ, Barg NL, Engleberg NC.** 1999. A two-component regulatory system, CsrR-CsrS, represses expression of three *Streptococcus pyogenes* virulence factors, hyaluronic acid capsule, streptolysin S, and pyrogenic exotoxin B. Infect. Immun. **67:**5298–5305.
19. **Federle MJ, McIver KS, Scott JR.** 1999. A response regulator that represses transcription of several virulence operons in the group A *Streptococcus*. J. Bacteriol. **181:**3649–3657.
20. **Treviño J, Perez N, Ramirez-Peña E, Liu Z, Shelburne SA, Musser JM, Sumby P.** 2009. CovS simultaneously activates and inhibits the CovR-mediated repression of distinct subsets of group A Streptococcus virulence factor-encoding genes. Infect. Immun. **77:**3141–3149. http://dx.doi.org/10.1128/IAI.01560-08.
21. **Aziz RK, Pabst MJ, Jeng A, Kansal R, Low DE, Nizet V, Kotb M.** 2004. Invasive M1T1 group A Streptococcus undergoes a phase-shift in vivo to prevent proteolytic degradation of multiple virulence factors by SpeB. Mol. Microbiol. **51:**123–134. http://dx.doi.org/10.1046/j.1365-2958.2003.03797.x.
22. **Engleberg NC, Heath A, Vardaman K, DiRita VJ.** 2004. Contribution of CsrR-regulated virulence factors to the progress and outcome of murine skin infections by Streptococcus pyogenes. Infect. Immun. **72:**623–628. http://dx.doi.org/10.1128/IAI.72.2.623-628.2004.
23. **Cole JN, McArthur JD, McKay FC, Sanderson-Smith ML, Cork AJ, Ranson M, Rohde M, Itzek A, Sun H, Ginsburg D, Kotb M, Nizet V, Chhatwal GS, Walker MJ.** 2006. Trigger for group A streptococcal M1T1 invasive disease. FASEB J. **20:**1745–1747. http://dx.doi.org/10.1096/fj.06-5804fje.
24. **Zhu H, Liu M, Sumby P, Lei B.** 2009. The secreted esterase of group A streptococcus is important for invasive skin infection and dissemination in mice. Infect. Immun. **77:**5225–5232. http://dx.doi.org/10.1128/IAI.00636-09.
25. **Liu M, Zhu H, Li J, Garcia CC, Feng W, Kirpotina LN, Hilmer J, Tavares LP, Layton AW, Quinn MT, Bothner B, Teixeira MM, Lei B.** 2012. Group A Streptococcus secreted esterase hydrolyzes platelet-activating factor to impede neutrophil recruitment and facilitate innate immune evasion. PLoS Pathog. **8:**e1002624. http://dx.doi.org/10.1371/journal.ppat.1002624.
26. **Engleberg NC, Heath A, Miller A, Rivera C, DiRita VJ.** 2001. Spontaneous mutations in the CsrRS two-component regulatory system of *Streptococcus pyogenes* result in enhanced virulence in a murine model of skin and soft tissue infection. J. Infect. Dis. **183:**1043–1054. http://dx.doi.org/10.1086/319291.
27. **Walker MJ, Hollands A, Sanderson-Smith ML, Cole JN, Kirk JK, Henningham A, McArthur JD, Dinkla K, Aziz RK, Kansal RG, Simpson AJ, Buchanan JT, Chhatwal GS, Kotb M, Nizet V.** 2007. DNase Sda1 provides selection pressure for a switch to invasive group A streptococcal infection. Nat. Med. **13:**981–985. http://dx.doi.org/10.1038/nm1612.
28. **Cole JN, Pence MA, von Köckritz-Blickwede M, Hollands A, Gallo RL, Walker MJ, Nizet V.** 2010. M protein and hyaluronic acid capsule are essential for in vivo selection of covRS mutations characteristic of invasive serotype M1T1 group A Streptococcus. mBio **1**(4)**:**e00191-10. http://dx.doi.org/10.1128/mBio.00191-10.
29. **Venturini C, Ong CL, Gillen CM, Ben-Zakour NL, Maamary PG, Nizet V, Beatson SA, Walker MJ.** 2013. Acquisition of the Sda1-encoding bacteriophage does not enhance virulence of the M1 Streptococcus pyogenes strain SF370. Infect. Immun. **81:**2062–2069. http://dx.doi.org/10.1128/IAI.00192-13.
30. **Tsatsaronis JA, Hollands A, Cole JN, Maamary PG, Gillen CM, Zakour NL, Kotb M, Nizet V, Beatson SA, Walker MJ, Sanderson-Smith ML.** 2013. Streptococcal collagen-like protein A and general stress protein 24 are immunomodulating virulence factors of group A Streptococcus. FASEB J. **27:**2633–2643. http://dx.doi.org/10.1096/fj.12-226662.
31. **National Research Council.** 2011. Guide for the care and use of laboratory animals, 8th ed. National Academies Press, Washington, DC.
32. **Ferretti JJ, McShan WM, Ajdic D, Savic DJ, Savic G, Lyon K, Primeaux C, Sezate S, Suvorov AN, Kenton S, Lai HS, Lin SP, Qian Y, Jia HG, Najar FZ, Ren Q, Zhu H, Song L, White J, Yuan X, Clifton SW, Roe BA, McLaughlin R.** 2001. Complete genome sequence of an M1 strain of Streptococcus pyogenes. Proc. Natl. Acad. Sci. U. S. A. **98:**4658–4663. http://dx.doi.org/10.1073/pnas.071559398.
33. **Cacalano G, Lee J, Kikly K, Ryan AM, Pitts-Meek S, Hultgren B, Wood WI, Moore MW.** 1994. Neutrophil and B cell expansion in mice that lack the murine IL-8 receptor homolog. Science **265:**682–684. http://dx.doi.org/10.1126/science.8036519.
34. **Ma Y, Bryant AE, Salmi DB, Hayes-Schroer SM, McIndoo E, Aldape MJ, Stevens DL.** 2006. Identification and characterization of bicistronic speB and prsA gene expression in the group A Streptococcus. J. Bacteriol. **188:**7626–7634. http://dx.doi.org/10.1128/JB.01059-06.
35. **Bradley PP, Priebat DA, Christensen RD, Rothstein G.** 1982. Measurement of cutaneous inflammation: estimation of neutrophil content with an enzyme marker. J. Investig. Dermatol. **78:**206–209. http://dx.doi.org/10.1111/1523-1747.ep12506462.
36. **Liu G, Liu M, Xie G, Lei B.** 2013. Characterization of streptococcal platelet-activating factor acetylhydrolase variants that are involved in innate immune evasion. Infect. Immun. **81:**3128–3138. http://dx.doi.org/10.1128/IAI.00398-13.
37. **Liu M, Hanks TS, Zhang J, McClure MJ, Siemsen DW, Elser JL, Quinn MT, Lei B.** 2006. Defects in ex vivo and in vivo growth and sensitivity to osmotic stress of group A Streptococcus caused by interruption of response regulator gene vicR. Microbiology **152:**967–978. http://dx.doi.org/10.1099/mic.0.28706-0.
38. **Daley JM, Thomay AA, Connolly MD, Reichner JS, Albina JE.** 2008. Use of Ly6G-specific monoclonal antibody to deplete neutrophils in mice. J. Leukoc. Biol. **83:**64–70. http://dx.doi.org/10.1189/jlb.0407247.
39. **Bos A, Wever R, Roos D.** 1978. Characterization and quantification of the peroxidase in human monocytes. Biochim. Biophys. Acta **525:**37–44. http://dx.doi.org/10.1016/0005-2744(78)90197-3.
40. **Tatsuno I, Okada R, Zhang Y, Isaka M, Hasegawa T.** 2013. Partial loss of CovS function in Streptococcus pyogenes causes severe invasive disease. BMC Res. Notes **6:**126. http://dx.doi.org/10.1186/1756-0500-6-126.
41. **Miyoshi-Akiyama T, Ikebe T, Watanabe H, Uchiyama T, Kirikae T, Kawamura Y.** 2006. Use of DNA arrays to identify a mutation in the negative regulator, csrR, responsible for the high virulence of a naturally occurring type M3 group A streptococcus clinical isolate. J. Infect. Dis. **193:**1677–1684. http://dx.doi.org/10.1086/504263.
42. **Horstmann N, Sahasrabhojane P, Suber B, Kumaraswami M, Olsen RJ, Flores A, Musser JM, Brennan RG, Shelburne SA, III.** 2011. Distinct single amino acid replacements in the control of virulence regulator protein differentially impact streptococcal pathogenesis. PLoS Pathog. **7:**e1002311. http://dx.doi.org/10.1371/journal.ppat.1002311.
43. **Mishalian I, Ordan M, Peled A, Maly A, Eichenbaum MB, Ravins M, Aychek T, Jung S, Hanski E.** 2011. Recruited macrophages control dissemination of group A Streptococcus from infected soft tissues. J. Immunol. **187:**6022–6031. http://dx.doi.org/10.4049/jimmunol.1101385.
44. **Edwards RJ, Taylor GW, Ferguson M, Murray S, Rendell N, Wrigley A, Bai Z, Boyle J, Finney SJ, Jones A, Russell HH, Turner C, Cohen J, Faulkner L, Sriskandan S.** 2005. Specific C-terminal cleavage and inactivation of interleukin-8 by invasive disease isolates of Streptococcus pyogenes. J. Infect. Dis. **192:**783–790. http://dx.doi.org/10.1086/432485.
45. **Zinkernagel AS, Timmer AM, Pence MA, Locke JB, Buchanan JT, Turner CE, Mishalian I, Sriskandan S, Hanski E, Nizet V.** 2008. The IL-8 protease SpyCEP/ScpC of group A Streptococcus promotes resistance to neutrophil killing. Cell Host Microbe **4:**170–178. http://dx.doi.org/10.1016/j.chom.2008.07.002.
46. **Sumby P, Zhang S, Whitney AR, Falugi F, Grandi G, Graviss EA, Deleo FR, Musser JM.** 2008. A chemokine-degrading extracellular protease made by group A Streptococcus alters pathogenesis by enhancing evasion of the innate immune response. Infect. Immun. **76:**978–985. http://dx.doi.org/10.1128/IAI.01354-07.
47. **Wexler DE, Chenoweth DE, Cleary PP.** 1985. Mechanism of action of the group A streptococcal C5a inactivator. Proc. Natl. Acad. Sci. U. S. A. **82:**8144–8148. http://dx.doi.org/10.1073/pnas.82.23.8144.
48. **Perez-Casal J, Caparon MG, Scott JR.** 1992. Introduction of the emm6 gene into an emm-deleted strain of *Streptococcus pyogenes* restores its ability to resist phagocytosis. Res. Microbiol. **143:**549–558. http://dx.doi.org/10.1016/0923-2508(92)90112-2.
49. **Ashbaugh CD, Moser TJ, Shearer MH, White GL, Kennedy RC, Wessels MR.** 2000. Bacterial determinants of persistent throat colonization and

the associated immune response in a primate model of human group A streptococcal pharyngeal infection. Cell. Microbiol. **2:**283–292. http://dx.doi.org/10.1046/j.1462-5822.2000.00050.x.

50. **Miyoshi-Akiyama T, Takamatsu D, Koyanagi M, Zhao J, Imanishi K, Uchiyama T.** 2005. Cytocidal effect of Streptococcus pyogenes on mouse neutrophils in vivo and the critical role of streptolysin S. J. Infect. Dis. **192:**107–116. http://dx.doi.org/10.1086/430617.
51. **Ato M, Ikebe T, Kawabata H, Takemori T, Watanabe H.** 2008. Incompetence of neutrophils to invasive group A *Streptococcus* is attributed to induction of plural virulence factors by dysfunction of a regulator. PLoS One **3:**e3455. http://dx.doi.org/10.1371/journal.pone.0003455.
52. **Timmer AM, Timmer JC, Pence MA, Hsu LC, Ghochani M, Frey TG, Karin M, Salvesen GS, Nizet V.** 2009. Streptolysin O promotes group A Streptococcus immune evasion by accelerated macrophage apoptosis. J. Biol. Chem. **284:**862–871. http://dx.doi.org/10.1074/jbc.M804632200.
53. **Lei B, DeLeo FR, Hoe NP, Graham MR, Mackie SM, Cole RL, Liu M, Hill HR, Low DE, Federle MJ, Scott JR, Musser JM.** 2001. Evasion of human innate and acquired immunity by a bacterial homolog of CD11b that inhibits opsonophagocytosis. Nat. Med. **7:**1298–1305. http://dx.doi.org/10.1038/nm1201-1298.
54. **Sumby P, Barbian KD, Gardner DJ, Whitney AR, Welty DM, Long RD, Bailey JR, Parnell MJ, Hoe NP, Adams GG, Deleo FR, Musser JM.** 2005. Extracellular deoxyribonuclease made by group A Streptococcus assists pathogenesis by enhancing evasion of the innate immune response. Proc. Natl. Acad. Sci. U. S. A. **102:**1679–1684. http://dx.doi.org/10.1073/pnas.0406641102.
55. **Schnitzler N, Haase G, Podbielski A, Lütticken R, Schweizer KG.** 1999. A co-stimulatory signal through ICAM-beta2 integrin-binding potentiates neutrophil phagocytosis. Nat. Med. **5:**231–235. http://dx.doi.org/10.1038/5597.
56. **Nizet V, Ohtake T, Lauth X, Trowbridge J, Rudisill J, Dorschner RA, Pestonjamasp V, Piraino J, Huttner K, Gallo RL.** 2001. Innate antimicrobial peptide protects the skin from invasive bacterial infection. Nature **414:**454–457. http://dx.doi.org/10.1038/35106587.
57. **DeMaster E, Schnitzler N, Cheng Q, Cleary P.** 2002. M(+) group A streptococci are phagocytized and killed in whole blood by C5a-activated polymorphonuclear leukocytes. Infect. Immun. **70:**350–359. http://dx.doi.org/10.1128/IAI.70.1.350-359.2002.
58. **Matsumura T, Ato M, Ikebe T, Ohnishi M, Watanabe H, Kobayashi K.** 2012. Interferon-γ-producing immature myeloid cells confer protection against severe invasive group A Streptococcus infections. Nat. Commun. **3:**678. http://dx.doi.org/10.1038/ncomms1677.
59. **Navarini AA, Lang KS, Verschoor A, Recher M, Zinkernagel AS, Nizet V, Odermatt B, Hengartner H, Zinkernagel RM.** 2009. Innate immune-induced depletion of bone marrow neutrophils aggravates systemic bacterial infections. Proc. Natl. Acad. Sci. U. S. A. **106:**7107–7112. http://dx.doi.org/10.1073/pnas.0901162106.
60. **Aziz RK, Kansal R, Aronow BJ, Taylor WL, Rowe SL, Kubal M, Chhatwal GS, Walker MJ, Kotb M.** 2010. Microevolution of group A streptococci in vivo: capturing regulatory networks engaged in sociomicrobiology, niche adaptation, and hypervirulence. PLoS One **5:**e9798. http://dx.doi.org/10.1371/journal.pone.0009798.
61. **Turner CE, Kurupati P, Jones MD, Edwards RJ, Sriskandan S.** 2009. Emerging role of the interleukin-8 cleaving enzyme SpyCEP in clinical Streptococcus pyogenes infection. J. Infect. Dis. **200:**555–563. http://dx.doi.org/10.1086/603541.
62. **Beres SB, Sylva GL, Barbian KD, Lei B, Hoff JS, Mammarella ND, Liu MY, Smoot JC, Porcella SF, Parkins LD, Campbell DS, Smith TM, McCormick JK, Leung DY, Schlievert PM, Musser JM.** 2002. Genome sequence of a serotype M3 strain of group A Streptococcus: phage-encoded toxins, the high-virulence phenotype, and clone emergence. Proc. Natl. Acad. Sci. U. S. A. **99:**10078–10083. http://dx.doi.org/10.1073/pnas.152298499.
63. **Green NM, Zhang S, Porcella SF, Nagiec MJ, Barbian KD, Beres SB, LeFebvre RB, Musser JM.** 2005. Genome sequence of a serotype M28 strain of group A streptococcus: potential new insights into puerperal sepsis and bacterial disease specificity. J. Infect. Dis. **192:**760–770. http://dx.doi.org/10.1086/430618.